Check for updates

Original Research Article

Narirutin Induces Cytotoxicity and Apoptosis in Gastric Cancer Cells Through Oxidative Stress Modulation

Pharmacognosy Magazine
22(3) 974–985, 2026
© The Author(s) 2025
Article reuse guidelines:
in.sagepub.com/journals-permissions-india
DOI: 10.1177/09731296251391926
journals.sagepub.com/home/phm
Sage

Zhongting Pan[1] and Yanling Guo[1]

Abstract

Background: Gastric cancer remains a major global health challenge, with approximately 1.1 million new cases and 770,000 deaths reported annually. Despite ongoing advancements in therapeutics, the prognosis for patients with advanced gastric cancer remains poor, underscoring the need for novel, safe, and effective treatment options. Natural flavonoids have gained increasing attention due to their multi-targeted mechanisms and low-toxicity profiles. Narirutin, a citrus-derived flavonoid glycoside, has been recognized for its antioxidant and anti-inflammatory activities; however, its direct anti-cancer potential in gastric cancer models remains underexplored.

Objectives: This study aims to investigate the anti-proliferative and apoptosis-inducing effects of narirutin in human gastric adenocarcinoma (AGS) cells, while also assessing its impact on oxidative stress and relevant molecular targets involved in apoptosis and inflammation.

Materials and Methods: AGS gastric cancer cells were treated with varying concentrations of narirutin. Cell viability was evaluated using the 3-(4,5-dimethylthiazol-2-yl)-2,5-diphenyltetrazolium bromide (MTT) assay. Apoptosis was assessed via acridine orange/ethidium bromide (AO/EB) staining, while intracellular reactive oxygen species (ROS) levels were measured using 2′,7′-dichlorodihydrofluorescein diacetate (DCFH-DA) staining. *In silico* molecular docking studies were conducted to predict narirutin's binding affinity toward key apoptotic (caspase-3 (CASP3), BCL2-associated X (BAX)) and inflammatory (nuclear factor kappa B subunit 1 (NF-κB1), nuclear factor kappa B subunit 2 (NF-κB2)) proteins, as well as glycolytic enzymes lactate dehydrogenase A (LDHA) and lactate dehydrogenase B (LDHB).

Results: Narirutin treatment led to a concentration-dependent reduction in AGS cell viability, with accompanying morphological features of apoptosis and elevated ROS levels. These findings suggest that narirutin may induce cancer cell death via a pro-oxidant mechanism. Docking studies supported these observations, revealing strong binding affinities with LDHA (−9.4 kcal/mol, 1.524 Å root mean square deviation (RMSD)) and LDHB (−8.7 kcal/mol, 2.449 Å RMSD), along with favorable interactions with CASP3, BAX, NF-κB1, and NF-κB2, indicating its potential to modulate key regulators of apoptosis and inflammation.

Conclusion: Nursing care is important in terms of educating patients about new treatments, providing support to patients participating in clinical trials, and providing counseling. The findings demonstrate that narirutin exerts pro-apoptotic and pro-oxidant effects on AGS gastric cancer cells, likely by interfering with redox homeostasis and inflammatory signaling pathways. These results provide a mechanistic rationale for further investigation of narirutin as an anti-cancer candidate for gastric cancer.

Keywords

Gastric cancer, human gastric cancer cell line cells, narirutin, apoptosis, cytotoxicity, reactive oxygen species, molecular docking

Received 25 April 2025; **revised** 26 July 2025; **accepted** 18 September 2025

Introduction

Gastric cancer is ranked globally as the fifth most unusual kind of malignancy and the third leading cause of the world's cancer-associated deaths, accounting for 1,000,000 reviews and 0.7 million deaths per keeping with 12 months (Sung et al., 2021). Despite advancements in remedy modalities

[1]Shanxi Bethune Hospital, Shanxi Academy of Medical Sciences, Third Hospital of Shanxi Medical University, Tongji Shanxi Hospital, Taiyuan, Shanxi, China

Corresponding author:
Yanling Guo, Shanxi Bethune Hospital, Shanxi Academy of Medical Sciences, Third Hospital of Shanxi Medical University, Tongji Shanxi Hospital, Taiyuan, Shanxi 030032, China.
E-mail: xldgg1@163.com

Creative Commons Non Commercial CC BY-NC: This article is distributed under the terms of the Creative Commons Attribution-NonCommercial 4.0 License (http://www.creativecommons.org/licenses/by-nc/4.0/) which permits non-Commercial use, reproduction and distribution of the work without further permission provided the original work is attributed as specified on the SAGE and Open Access pages (https://us.sagepub.com/en-us/nam/open-access-at-sage).

such as surgical treatment, chemotherapy, and immunotherapy, the viable remedy for advanced gastric cancer remains unfavorable, with a typically low survival rate (<30%) in the majority of instances (Bray et al., 2020). The complexity of gastric cancer's molecular pathogenesis and the challenges posed by its heterogeneity keep obstructing the improvement of powerful remedies. As a result, there may be a growing need for novel and extra-centered approaches to supplement present treatments and probably improve survival outcomes for sufferers with advanced degrees of this disease.

Apoptosis, which refers to programmed cell death, is vital for homeostasis and an important goal in most cancer remedies (Elmore, 2007). Dysregulation of apoptotic pathways allows cancer cells to avoid dying, main to out-of-control proliferation. In most cancer cells, the balance of signaling mediators involved before and against apoptosis is frequently disturbed, facilitating tumorigenesis and resistance to standard remedies. The apoptotic intrinsic pathway, regulated with the aid of the interaction of Bcl-2, determines the fate of the cellular (Czabotar et al., 2014). Whereas Bcl-2 opposes this process, many pro-apoptotic proteins assist in substrate transport into the mitochondria (Youle & Strasser, 2008). Primary to apoptosis execution via cleavage of cellular substrates and deoxyribonucleic acid (DNA) damage are the caspases, notably caspase-3 (CASP3) (Galluzzi et al., 2018). In gastric cancer cells, interruption of apoptotic pathways causes the avoidance of this essential cell death mechanism, therefore advancing the disease.

Novel methods are particularly needed to selectively hit cancer cells while reducing general toxicity, given the restrictions of existing treatment options. The desperate demand for fresh medical treatments has focused interest on bioactive natural chemicals that could target cancer cells with little side effects (Naeem et al., 2022). Cancer research is increasingly turning toward natural compounds, known for their multi-targeted actions and lower toxicity (Shi et al., 2015). A phytochemical synthesized in citrus fruits, narirutin, is a flavanone glycoside that shows an array of biological properties such as anti-inflammatory, antioxidant, and anti-cancer activities. Recent studies highlight the potential of narirutin to affect major processes that facilitate the spread of tumors.

Narirutin, the most abundant bioactive compound found in citrus fruits as a glycoside flavonoid, has gained considerable interest due to its numerous biological activities (Huang et al., 2017). It has been documented that narirutin possesses antioxidant and anti-inflammatory properties due to the early quenching of reactive oxygen species (ROS) and modification of inflammation-mediated signaling pathways. Its anticancer properties have been reported for many different tumors, including colorectal, prostate, and breast cancers (Chen et al., 2019). These observations are linked to its pharmacognostic properties, which modulate the cell signal transduction pathways. Recently, alongside narirutin, some studies have investigated the apoptosis-targeting potential of flavonoid compounds, thus exploring their anti-cancer efficacy. For example, it was mentioned that narirutin triggered apoptosis in hormone-resistant prostate cancer cells by activating CASP3 and affecting Bcl factors (Zhou, Liu, et al., 2020; Zhou, Zhang, et al., 2020). However, limited research exists on its impact on gastric cancer cells; hence, further research is necessary. However, the anti-cancer effect of narirutin on gastric cancer cells is not well understood yet, so further research into its potential application as an anti-cancer treatment for this type of cancer is warranted.

One of the biggest problems with the treatment of stomach cancer is its late diagnosis stage and generally unsatisfactory patient outcomes because of limited therapy options. Chemotherapy and radiation therapy are usually given, even though they do not always effectively treat tumors, and extreme side effects accompany them. In this case, examining the effects of organic compounds such as narirutin makes it possible to find substitutes that are much less harmful and can aid in therapies. Moreover, understanding the molecular pathways of apoptosis in gastric cancer cells may reveal new precision medicine targets, useful as therapeutic targets, and relevant novel biomarkers (Rauf et al., 2022).

With the limitations of current therapies, bioactive natural products such as narirutin have been of interest for their potential anti-cancer properties. Flavonoid narirutin, predominantly found in citrus fruits, has been reported in several cancers—such as prostate, colorectal, and breast cancers—with antioxidant, anti-inflammatory, and pro-apoptotic activities (Ganesh et al., 2023). Yet to be explored is its effect on stomach cancer. This analysis suggests further research is necessary to assess narirutin's impact on the apoptotic pathways of gastric cancer cells. Given its ability to modulate critical processes involving homeostasis, apoptosis, and the generation of ROS, the compound stands out as a promising candidate for therapeutic applications. Given the risks of toxicity associated with current treatment options, compounds such as narirutin may provide a targeted, less hazardous means of treatment when used in conjunction with existing therapies (Massaro et al., 2023). Further research on the molecular mechanisms underlying the action of narirutin in gastric cancer cells, along with an exploration of its potential applications in evidence-based nursing care, may advance the development of precision medicine strategies.

This study attempts to evaluate the apoptotic effects of narirutin on gastric cancer cells utilizing *in vitro* techniques. More specifically, we focus on cell death, cleaved CASP3 activity, cell viability, apoptotic cellular shape, and the total oxidant status of the cell, which are all parameters of oxidative stress. This research seeks to develop novel therapeutic strategies for managing stomach cancer by revealing the biological basis of apoptosis caused by narirutin treatment.

Materials and Methods

Chemicals

The research utilized the following supplies: 2′,7′-dichlorodihydrofluorescein diacetate (DCFH-DA), phosphate-buffered

saline (PBS), ethidium bromide (EB), acridine orange (AO), lactate dehydrogenase (LDH) reaction mixture, a microplate reader, 3-(4,5-dimethylthiazol-2-yl)-2,5-diphenyltetrazolium bromide (MTT) solution, dimethyl sulfoxide (DMSO), 96-well plates, an incubator, human gastric cancer cell line (AGS) cells, Dulbecco's modified Eagle medium (DMEM), fetal bovine serum (FBS), streptomycin-penicillin solution, dimethicone, a fluorescence plate reader, and serum-free medium.

Using Cells In Vitro

Subculture AGS cells were kept in a 37°C, 5% CO_2-incubator. Cells were cultured in DMEM, fortified with 1% anti-biotic-anti-mycotic solution (streptomycin and penicillin) and 10% FBS. The cells were roughly 70% confluent at the time of testing.

MTT Assay for Cytotoxicity Evaluation

The cytotoxic effects of narirutin on AGS cells were assessed using the MTT assay. Cells were seeded at a density of 5×10^3 cells/well in 96-well plates in DMEM containing 10% FBS, and incubated overnight. The cells were then treated with increasing concentrations of narirutin (10, 20, 30, 40, 50, and 60 μM) for 24 h. A control group receiving only the vehicle (DMSO <0.1%) without narirutin was maintained. After incubation, 20 μL of a 5 mg/mL MTT solution was added to each well and incubated for an additional 4 h at 37°C. The medium was removed, and the resulting formazan crystals were dissolved in 100 μL of DMSO. Absorbance was measured at 490 nm using a microplate reader (BioTek, USA). Experiments were performed in triplicate, and cell viability (%) was calculated as: Cytotoxicity (%) = (1 – Absorbance of treated cells/Absorbance of control cells) × 100 (Munusamy et al., 2025).

LDH Release Assay

To assess membrane integrity and cytotoxicity, the LDH activity assay was performed. AGS cells were plated at a density of 1×10^3 cells/well in 96-well plates and treated with narirutin at concentrations of 10–60 μM for 24 h. Post-treatment, culture supernatants were collected and mixed with the LDH reaction mixture (provided by the assay kit) according to the manufacturer's protocol. The plates were incubated for 30 min in the dark at room temperature, followed by the addition of the stop solution. Absorbance was measured at 490 nm, and LDH release was expressed as: Cytotoxicity (%) = (Sample LDH release/Total LDH release) × 100. All treatments were carried out in triplicate (Subbarayan et al., 2019).

AO/EB Dual Staining for Apoptosis Detection

Apoptotic morphological changes were assessed by AO/EB staining. AGS cells were seeded in 6-well plates (2×10^4 cells/well) and treated with narirutin for 24 h. After treatment, cells were washed twice with PBS and stained with 100 μg/mL AO/EB mixture for 10 min in the dark. Cells were visualized under a fluorescence microscope (Olympus BX51), and at least 300 cells per group were counted in randomly selected fields. Green fluorescent nuclei indicate live cells, orange/yellow indicate apoptotic cells, and red indicates necrotic cells. The apoptotic index (%) was calculated as the number of apoptotic cells divided by the total number of counted cells (Subbarayan et al., 2016).

Intracellular ROS Measurement by DCFH-DA Assay

Intracellular ROS levels were determined using DCFH-DA. AGS cells were cultured in black 96-well plates at 5×10^3 cells/well. Cells were first incubated with 10 μM DCFH-DA in serum-free medium for 30 min at 37°C in the dark to allow probe internalization. After washing off the excess dye with PBS, the cells were treated with various concentrations of narirutin for 24 h. Fluorescence was measured at an excitation wavelength of 485 nm and an emission at 528 nm using a microplate fluorometer. Data were collected from three independent experiments, each performed in triplicate (Munusamy et al., 2025).

Statistical Analysis

All data are expressed as Mean ± Standard Error of the mean (SEM) from at least three independent experiments. Statistical analysis was performed using one-way analysis of variance (ANOVA), followed by Tukey's *post hoc* test for multiple comparisons. A p value of <.05 was considered statistically significant. GraphPad Prism (version 10, GraphPad Software, USA) was used for data analysis and visualization.

In Silico Analysis

The targets 3D structures, such as LDHA (lactate dehydrogenase A), LDHB (lactate dehydrogenase B), CASP3, BAX (BCL2-associated X), NF-κB1 (nuclear factor kappa B subunit 1), and NF-κB2 (nuclear factor kappa B subunit 2), were obtained from the Protein Data Bank (PDB). The LDHA (PDB ID: 4QT0) (Kolappan et al., 2015), LDHB (PDB ID: 7DBJ) (Shibata et al., 2021), CASP3 (PDB ID: 3KJF) (Wang et al., 2010), BAX (PDB ID: 4BD7) (Czabotar et al., 2013), NF-κB1 (PDB ID: 1SVC) (Müller et al., 1995), and NF-κB2 (PDB ID: 7CLI) (Pan et al., 2023) were retrieved from the PDB (https://www.rcsb.org/) to identify the interactions with the narirutin using a molecular docking approach.

Preparation of Protein Structures and Ligands

The PDB provided the protein structures of LDHA, LDHB, CASP3, BAX, NF-κB1, and NF-κB2, and the water molecules and ligands were cleaned using Discovery Studio

Visualizer (DSV) v19.1.0.18287 (www.accelerys.com), and targets were built. Subsequently, narirutin's structure was downloaded from the PubChem compound database (https://pubchem.ncbi.nlm.nih.gov/) in the SDF format containing 3D coordinates (Kim et al., 2023) and converted to the PDB format via DSV.

Molecular Docking and Visualization

The molecular docking procedures for the targets LDHA, LDHB, CASP3, BAX, NF-κB1, and NF-κB2 with narirutin were conducted using Autodock Vina, a sophisticated scoring system contained in the PyRx software, which scores the docking results through a scoring function (Eberhardt et al., 2021). This process predicts the most favorable binding modes between the defined targets and narirutin.

The Autodock Vina Uses a New Scoring Mechanism

C—Sum of intermolecular and intramolecular distance; ∑—Over all of the pairs of atoms; ftitj—Symmetric set of interaction functions; rij—Interatomic distance.

The defined targets and narirutin have been converted into PDBQT format and were implemented using the blind docking approach set with an exhaustiveness of eight. Additionally, the properties of the grid box size were set to LDHA (x = 54.47 Å, y = 99.86 Å, z = 70.35 Å), LDHB (x = 65.12 Å, y = 66.06 Å, z = 102.28 Å), CASP3 (x = 54.05 Å, y = 69.66 Å, z = 60.41 Å), BAX (x = 48.42 Å, y = 88.32 Å, z = 56.23 Å), NF-κB1 (x = 88.09 Å, y = 78.33 Å, z = 72.73 Å), and NF-κB2 (x = 57.13 Å, y = 102.26 Å, z = 76.69 Å). With these parameters, we performed docking and analyzed the defined targets' interactions with narirutin in 3D and 2D using DSV v19.1.0.1828, developed by Dassault Systèmes BIOVIA. This software is available at Rue Marcel Dassault, Vélizy-Villacoublay, France (URL: www.accelerys.com, Accessed on March 8, 2025) (Asiri et al., 2025).

Statistical Analysis

Every experiment was conducted in triplicate, and the data were reported with the mean and standard deviation for each assay. Linear regression was used to determine the half-maximal inhibitory concentration (IC_{50}) value. To evaluate the data statistically, *post hoc* Tukey's tests and one-way ANOVA were employed. $p < .05$ was used to indicate significance.

Results

Cytotoxicity Effect of Narirutin on AGS Cells

MTT assay was employed to assess the cytotoxic effect of narirutin on AGS cells. The results, shown in Figure 1, demonstrate that there is a decrease in the viability of AGS cells with increasing concentrations of narirutin treatment. The IC_{50} value for narirutin was calculated to be 43 µM. At concentrations of 10–60 µM, cell viability decreased progressively, with the most notable reduction occurring at the highest concentration after 24 h of treatment.

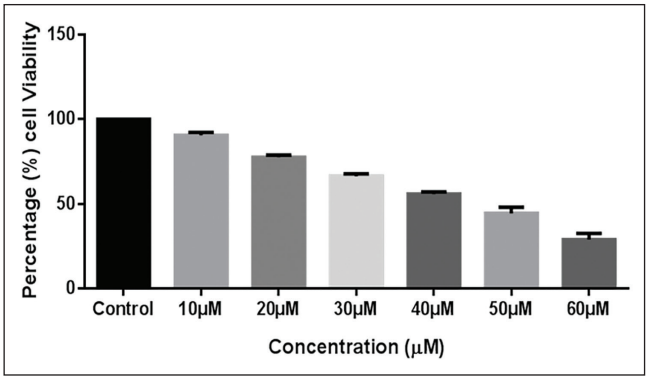


Figure 1. Impact of Narirutin on the Viability of Human Gastric Cancer Cell Line (AGS) Gastric Cancer Cells. At Concentrations Between 10 and 60 µM/mL, Narirutin had a Significant Impact on Reducing the Viability of AGS Cells, Reflecting Its Cytotoxicity.

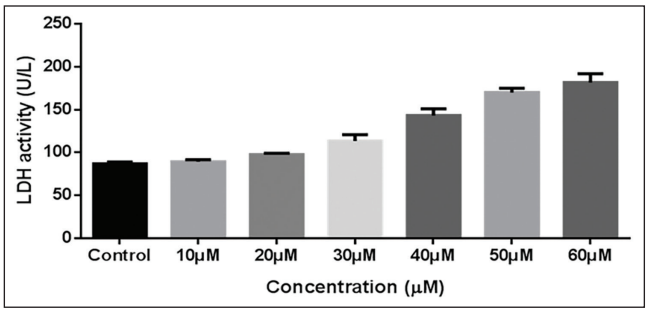


Figure 2. The Lactate Dehydrogenase (LDH) Activity in the Cell Culture Medium was Examined to Evaluate Cell Damage. We Study the Values Using GraphPad Software. Results are Presented as a Standard Deviation of Three Samples.

Effects of Narirutin on LDH Activity in AGS Cells

The LDH activity assay was performed to determine the impact of narirutin on cell membrane integrity in AGS cells. The results, shown in Figure 2, reveal that narirutin treatment led to a dose-dependent increase in LDH release, indicating damage to the cell membrane. The highest concentrations (50 and 60 µM) induced a significant increase in LDH activity, which was statistically higher compared to the control group, suggesting enhanced cytotoxicity at higher doses of narirutin.

Narirutin-induced Apoptotic Cell Death in AGS Cells

The AO/EB staining assay was used to determine the apoptotic induction potential of narirutin on AGS cells. Narirutin

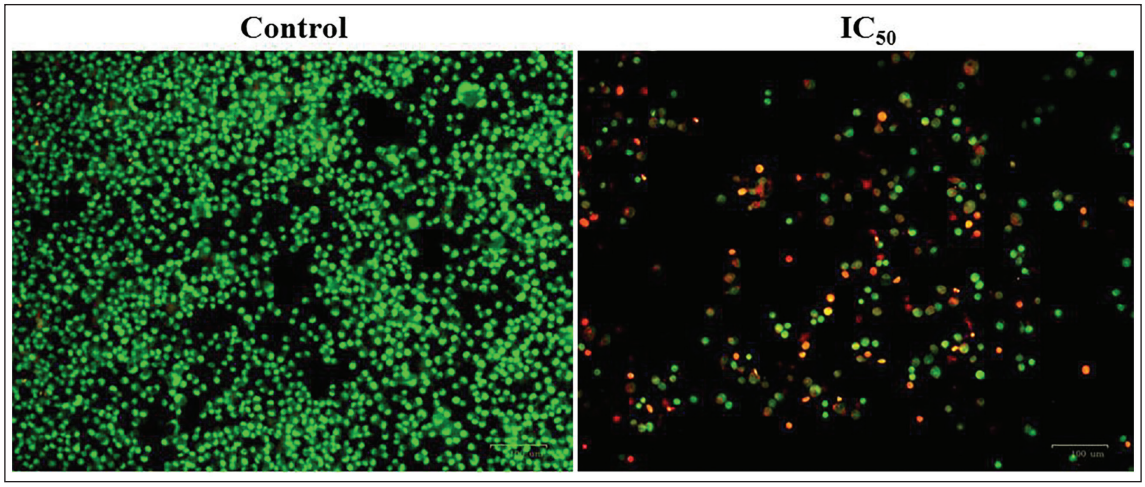


Figure 3. Effect of Narirutin on the Apoptotic Cell Death in the Human Gastric Cancer Cell Line (AGS) Cells. AGS Cells Showed Increased Yellow and Orange Fluorescence After Being Treated with Narirutin Half-maximal Inhibitory Concentration (IC_{50}) Values, Suggesting the Existence of Both Early and Late Apoptotic Cell Death.

treatment induced apoptosis, which was characterized by orange nuclei with condensed chromatin. Quantification of the apoptotic cells revealed that there was a significant dose-dependent increase in the percentage of apoptotic cells with increasing concentrations of narirutin treatment. Narirutin causes apoptosis in AGS cells, distinctive by the fact that a notable number of cells at 43 µM had apoptotic features (Figure 3).

AGS Cells ROS Formation Due to Narirutin

ROS production was measured using the DCFH-DA method. The findings show a marked rise in the levels of ROS with rising doses of narirutin therapy. The high fluorescence intensity observed in cells treated with 43 µM narirutin indicated a large rise in ROS. This would seem to show that narirutin causes oxidative stress in AGS cells, therefore helping its cytotoxic and apoptotic properties (Figure 4).

Molecular Docking Analysis

The molecular docking analysis performed for LDHA, LDHB, CASP3, BAX, NF-κB1, and NF-κB2 showed that narirutin can interact with all these defined targets, which might hinder the cell proliferation processes. The resulting binding affinity, root mean square deviation (RMSD), and the types of bonds formed between the defined targets and narirutin were tabulated in Table 1.

LDHA

The narirutin interacted with the residues of LDHA, including ASN164(2), ARG169, and ARG171(2), via hydrogen bonds and carbon–hydrogen bonds formed with SER167, ARG269, and PRO272. Additionally, the residues such as ALA168, ARG169, ARG171pA, ALA251, and TRP188 interacted via pi-alkyl, alkyl, and pi-sigma. Also, the hydrophobic residues such as LEU165, SER167, TYR172, HIS181, PRO182, LEU183, GLY187, SER237, LEU254, ARG269, VAL270, and HIS271 surrounded the complex with the binding affinity of −9.4 kcal/mol and 1.524 Å through the van der Waals interactions (Figure 5A, 5B, and Table 1).

LDHB

LDHB residues ARG172 and HIS272 interacted with the narirutin via hydrogen bonds, and other residues, such as ALA169, ARG170, and PRO183, bonded via pi-alkyl bonds. The residue TYR173 formed a carbon-hydrogen, pi-pi-T-shaped bond with narirutin. Also, residues such as ASN165, SER168, HIS182, PRO183, SER184, TRP189, ALA252, LEU255, SER256, ASP259, ARG270, ILE271, and PRO273 surrounded the complex with a binding affinity of −8.7 kcal/mol and an RMSD of 2.449 Å (Figure 5C, 5D and Table 1).

CASP3

The narirutin interacted with residues TYR37, ASP135, THR140, ARG144, GLY145, PRO155, LEU157, and ILE160 via hydrogen bonds. Additionally, the carbon-hydrogen, pi-pi-T-shaped, and pi-alkyl bonds formed with the residues LYS156, PHE158, LEU136, and LYS137. Also, the hydrophobic residues PHE143, LYS154, LYS156, GLY125, and PHE158 surrounded the complex with a binding affinity of −6.8 kcal/mol and the RMSD of 2.274 Å (Figure 5E, 5F and Table 1).

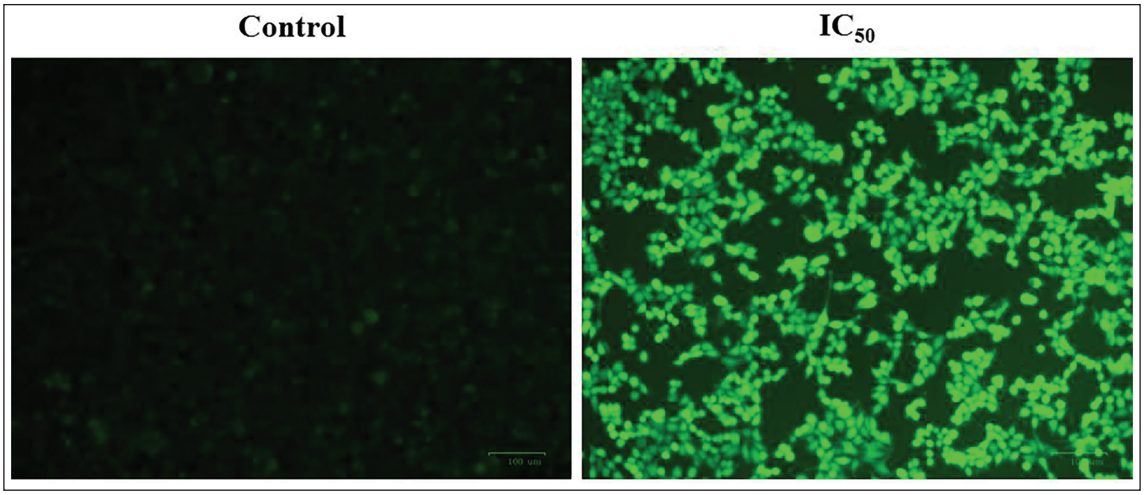


Figure 4. Fluorescence Microscope Image of Cells Treated with Narirutin and Stained with 2′,7′-Dichlorodihydrofluorescein Diacetate (DCFH-DA), Induced to Produce Intracellular Reactive Oxygen Species (ROS). Control Cells were Treated with Half-maximal Inhibitory Concentration (IC_{50}) Narirutin. A Representative Image of a Triplicate Experiment is Shown Here.

BAX

The narirutin interacted well with BAX residues that include ASP86, SER87(2), and PRO88 via hydrogen bonds, and ALA117, LYS128, ARG89, and PHE92(2) via alkyl, pi-alkyl, and pi-pi-T-shaped bonds. Also, the residues such as LEU27, THR85, VAL91, PHE93, LEU113, PHE114, LEU120, VAL121, ALA124, and LEU125 surrounded the complex via van der Waals forces with the binding affinity of −6.8 kcal/mol and 2.345 Å (Figure 5G, 5H and Table 1).

NF-κB1

The NF-κB1 interacted better with the narirutin (Figure 5I, 5J and Table 1). The narirutin significantly interacted with the residues GLY69, SER243, and ASN250(2), via four hydrogen bond interactions, with a binding affinity of −7.9 kcal/mol. The RMSD was observed as 2.414 Å. Also, the residues such as PHE56, PRO71, ARG57, LYS244, and LYS275 via the pi-alkyl, alkyl, and pi-pi-T-shaped bonds. Likely, the residues such as LYS52, GLY55, ARG59, HIS67, GLY68, LYS80, SER249, ASP274, and PHE310 were surrounded the complex via van der Waals interactions.

NF-κB2

Narirutin interacted with NF-κB2 by forming hydrogen bonds with GLU92, LEU117, ARG156, GLN157, and ARG193 residues. Meanwhile, alkyl, pi-alkyl, and pi-cation bonds are formed with the residues PRO211, ARG160, ARG160, GLN157, and other residues ASP94, ALA104, SER115, ILE119, LYS153, PHE197, PRO208, LEU209, and LYS210 are interacted with narirutin via van der Waals forces, with the binding affinity of −7.4 kcal/mol, and the RMSD was observed as 2.822 Å (Figure 5K, 5L and Table 1).

Discussion

As one of the most pervasive public health problems worldwide, gastric cancer is associated with high death rates. While numerous treatments are approved by the Food and Drug Administration (FDA), such as fluorouracil, trastuzumab, and pembrolizumab, and appear to be effective to some degree, they often do not extend life for long, especially in the advanced stages of the disease. Thus, there is an urgent need to develop new therapeutic agents that can selectively attack gastric cancer cells to improve treatment outcomes. Some flavonoids, including narirutin, have gained attention due to their claimed anti-cancer effects because of their antioxidant, anti-inflammatory, and pro-apoptotic activities. We carried out *in vitro* experiments to determine the cytotoxic activity, apoptotic activity, and oxidative stress response of narirutin in AGS gastric cancer cells. Earlier studies reported that cancer is a deadly disease, and the study explores prognostic biomarkers and identifies lepitaprocerin D as a potential inhibitor for BUB1B, a potential drug candidate for controlling breast cancer metastasis (Mishra et al., 2022). In previous studies, chemotherapeutics are needed due to the rising cancer burden, but there is a promising alternative for oncogenes like c-MYC. Recent advances in developing small compounds that selectively bind to and stabilize c-MYC G-quadruplexes (G4) have shown promise for inhibiting c-MYC signaling and tumor growth (Thumpati et al., 2025).

Future research should focus on more efficient cultivation methods and deeper exploration of fungal endophytes' genetic and metabolic capabilities to fully harness their therapeutic potential (Prajapati et al., 2025).

Based on the MTT assay, narirutin was found to decrease the viability of gastric cancer (AGS) cells at a 43 μM concentration, whose IC_{50} was determined to be 43 μM. Our findings demonstrate that narirutin triggers cytotoxicity and apoptosis

Table 1. List of Targets, Protein Data Bank (PDB) ID, Binding Affinity (kcal/mol), Root Mean Square Deviation (RMSD) (Å), and Their Interacted Residues with Narirutin and Its Type of Bonds.

Targets Name	Targets (PDB ID)	Binding Affinity (Kcal/mol)	RMSD (Å)	Hydrogen Bonds	Hydrophobic Residues	Other Types of Bonds
LDHA	4QT0	−9.4	1.524	ASN164(2), ARG169, ARG171(2).	LEU165, SER167, TYR172, HIS181, PRO182, LEU183, GLY187, SER237, LEU254, ARG269, VAL270, HIS271.	SER167^{CH}, ARG269^{CH}, PRO272^{CH}, ALA168^{A}, ARG169^{PA}, ARG171p^{A}, ALA251^{A}, TRP188^{PS}
LDHB	7DBJ	−8.7	2.449	ARG172, HIS272.	ASN165, SER168, HIS182, PRO183, SER184, TRP189, ALA252, LEU255, SER256, ASP259, ARG270, ILE271, PRO273.	TYR173$^{CH\|PPTS}$, ALA169^{PA}, ARG170^{PA}, PRO183^{PA}
CASP3	3KJF	−6.8	2.274	TYR37, ASP135, THR140, ARG144, GLY145, PRO155, LEU157, ILE160.	PHE143, LYS154, LYS156, GLY125, PHE158.	LYS156^{CH}, PHE158^{PPTS}, LEU136^{PA}, LYS137^{PA}
BAX	4BD7	−6.8	2.345	ASP86, SER87(2), PRO88.	LEU27, THR85, VAL91, PHE93, LEU113, PHE114, LEU120, VAL121, ALA124, LEU125.	ALA117^{A}, LYS128^{PA}, ARG89^{PS}, PHE92(2)^{PPTS}
NF-κB1	1SVC	−7.9	2.414	GLY69, SER243, ASN250(2).	LYS52, GLY55, ARG59, HIS67, GLY68, LYS80, SER249, ASP274, PHE310.	PHE56^{PPTS}, PRO71^{A}, ARG57^{A}, LYS244^{PA}, LYS275^{UFDD}
NF-κB2	7CLI	−7.4	2.822	GLU92, LEU117, ARG156, GLN157, ARG193.	ASP94, ALA104, SER115, ILE119, LYS153, PHE197, PRO208, LEU209, LYS210.	PRO211^{A}, ARG160^{PA}, ARG160^{PC}, GLN157^{UFDD}

Note: BAX: BCL2-associated X; CASP3: Caspase-3; LDHA: Lactate dehydrogenase A; LDHB: Lactate dehydrogenase B; NF-κB1: Nuclear factor kappa B subunit 1; NF-κB2: Nuclear factor kappa B subunit 2; PA: Pi alkyl; PPT: Pi-Pi T-shaped.

in gastric cancer cells via oxidative stress modulation. These results align with previous investigations reporting the anticancer properties of flavonoids and narirutin in particular across various models (Zhang et al., 2017). This decreased viability suggests that narirutin may promote apoptosis while preventing metastasis, and thus becomes a candidate for further therapeutic validation. Since narirutin therapy resulted in a dose-dependent rise in LDH release, the LDH activity test also confirmed the cytotoxicity results. Zhou, Liu, et al. (2020) and Zhou, Zhang, et al. (2020) point out that LDH release into the culture medium helps to indicate cell damage or death. The compound seems to cause cell membrane damage, resulting in the observed cytotoxic effects, given the strong rise in LDH levels at higher concentrations of narirutin.

Designated by the orange nuclei with compact chromatin, the apoptotic cell death assay, done using AO/EB staining, showed that narirutin initiated apoptosis in AGS cells. These are consistent with narirutin's pro-apoptotic features researched earlier in several cancer cell lines (Pachauri et al., 2018). The dose-dependent rise in apoptotic cells provides more evidence in favor of the theory that narirutin induces cell death via apoptosis, a desirable mechanism for anti-cancer treatment. DCFH-DA staining showing ROS detection found that narirutin treatment significantly raises intracellular ROS levels, thereby implying that narirutin increases AGS cell oxidative stress. By destroying cellular parts and, hence, autophagy, oxidative stress is vital in cancer cell death (Cai et al., 2018). The observed rise in intracellular ROS levels suggests a key mechanistic role in mediating narirutin's anticancer activity, likely through oxidative stress-induced cell death. Our results indicate that ROS generation occurs before the onset of apoptotic features, such as chromatin condensation and membrane blebbing, implying that oxidative stress

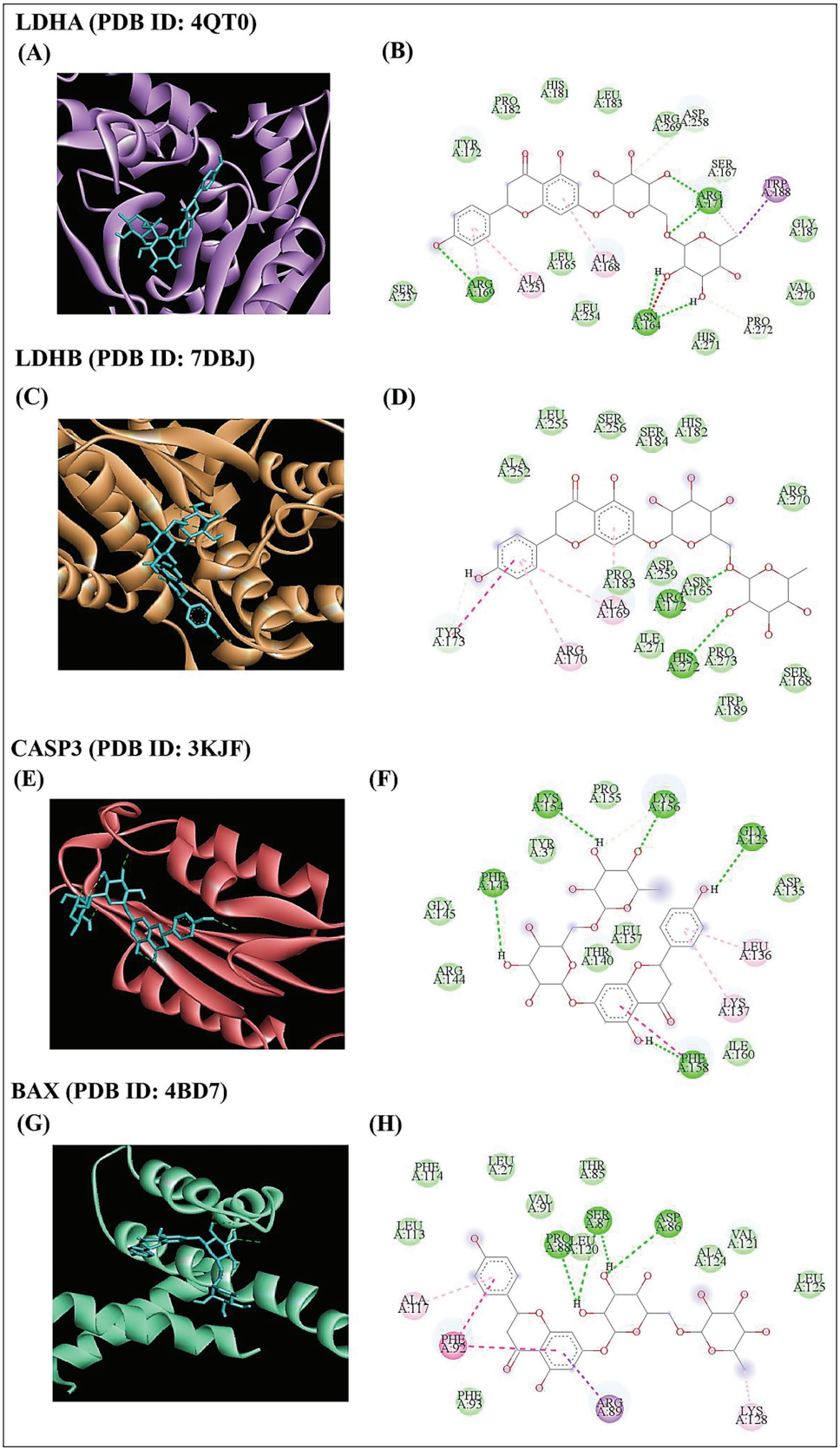


Figure 5. *(continued)*.

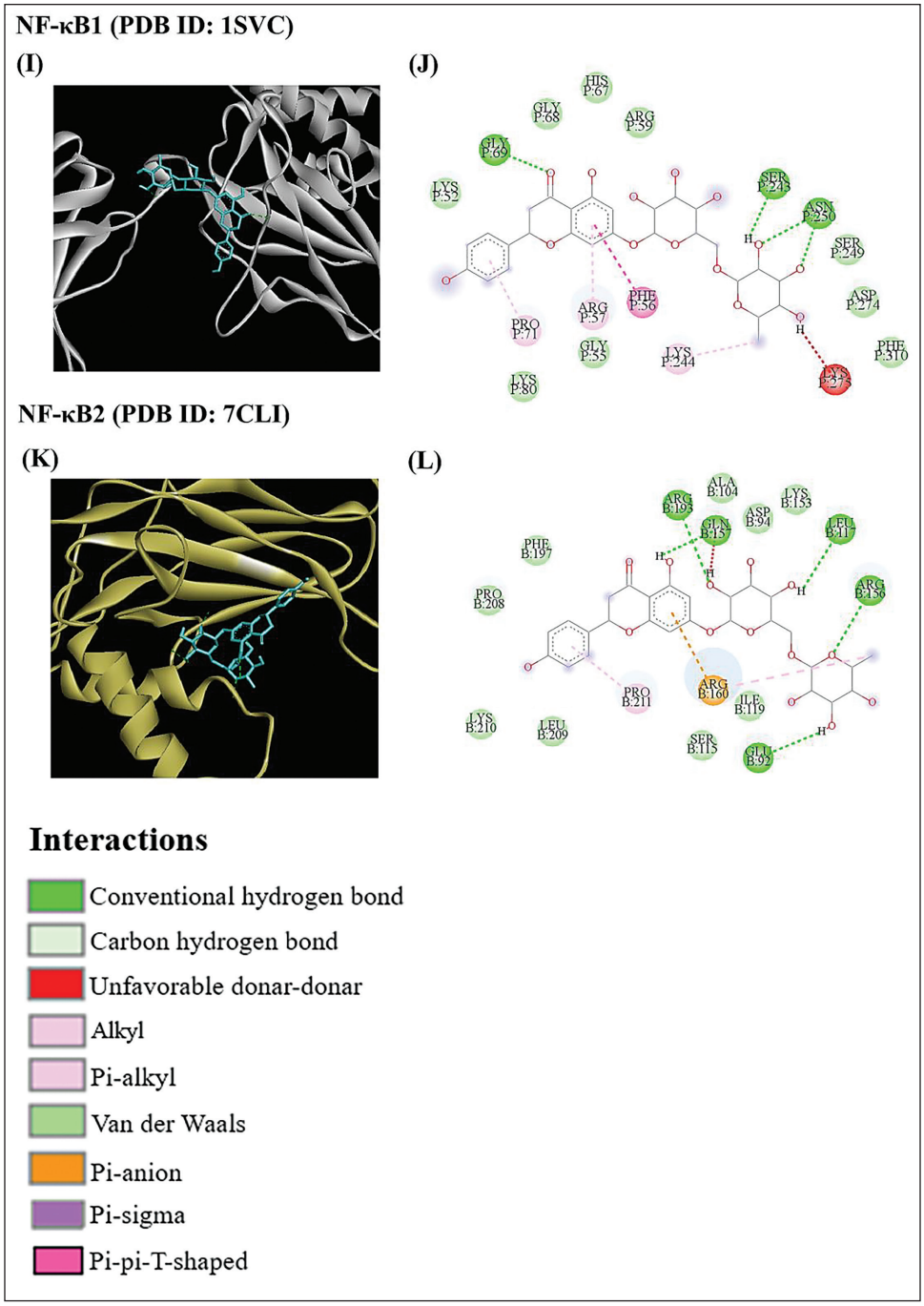


Figure 5. The Docking 3D and 2D Poses of the Defined Targets Lactate Dehydrogenase A (LDHA) (A, B), Lactate Dehydrogenase B (LDHB) (C, D), Caspase-3 (CASP3) (E, F), BCL2-associated X (BAX) (G, H), Nuclear Factor Kappa B Subunit 1 (NF-κB1) (I, J), and Nuclear Factor Kappa B Subunit 2 (NF-κB2) (K, L) with Narirutin.

may act as an upstream trigger for apoptosis. Similar mechanisms have been reported in previous studies, where ROS was identified as a crucial initiator of mitochondrial dysfunction and caspase activation in cancer cells (Nakamura & Takada, 2021). However, to establish a definitive causal relationship, further validation using ROS scavengers such as *N*-acetylcysteine (NAC) is necessary, as demonstrated in prior investigations on flavonoid-induced apoptosis (Liu et al., 2023).

Recent research has been looking for similarly possible phytochemicals to narirutin, like naringin and naringenin (NG). Via several cell signal transduction pathways, they have demonstrated anti-carcinogenic events. When used together with typical anti-cancer drugs, these chemicals have

shown synergistic effects that outperform monotherapy. Moreover, they help cancer therapy fight a major obstacle, multidrug resistance. NG and naringenin-7-*O*-glucoside (NGE) have been thoroughly investigated for their roles in cancer treatment, given their ability to improve the efficiency of current treatments. Further study and development of promising anti-cancer compounds, such as narirutin, might be found in the derivatives of these molecules.

Particularly in late stages, gastric cancer is a leading cause of mortality for cancer, with little survival advantage from present therapies. The search for novel, powerful treatments has redoubled; natural substances such as narirutin are great candidates thanks to their many bioactivities. In gastric cancer cells, this study shows narirutin's cytotoxic agent potential, since it causes dose-dependent cell viability reductions and apoptosis. In line with prior observations in several types of cancer, the MTT and LDH assays confirmed narirutin cytotoxicity, utilizing elevated cell membrane destruction and cell death. AO/EBD staining also confirmed the apoptotic induction, thereby emphasizing letiriruitin's ability to activate apoptosis via nuclear fragmentation and chromatin condensation. The strong increase in ROS levels shows the sequestering oxidative stress, therefore revealing its mechanism of action.

The molecular docking results revealed that narirutin exhibited better binding affinity for the key cancer-associated proteins, including LDHA, LDHB, CASP3, BAX, NF-κB1, and NF-κB2. LDHA (−9.4 kcal/mol) and LDHB (−8.7 kcal/mol) demonstrated the highest binding affinities, suggesting that narirutin may be crucial in altering metabolic pathways involved in cancer cell proliferation. The earlier report described LDHA and LDHB as triggering tumor development by inducing the Warburg effect. Meanwhile, LDHA and LDHB increased hydrogen peroxide levels in tumor cells, which enhanced oxidative stress, cell adhesion, and transcribing genes related to the cancer cells' proliferation and division (Wu et al., 2021). The results suggest that narirutin-induced LDH activity might be associated with metabolic disruption, oxidative stress, and apoptosis in AGS cells. However, enzymatic assays are required to confirm the narirutin's role in inhibiting LDHA and LDHB activity in the future. Furthermore, narirutin interacted with the key apoptotic proteins CASP3 and BAX, indicating that it promotes apoptotic signaling, which may increase cell death. Additionally, significant binding affinities were observed with NF-κB1 (−7.9 kcal/mol) and NF-κB2 (−7.4 kcal/mol), indicating that narirutin could modulate the inflammation-associated cancer pathways. Xia et al. (2014) reported that NF-κB acts as an active player in human cancer by exhibiting inflammatory responses, cell survival and proliferation.

This study was intended as a preliminary evaluation of the anti-cancer potential of narirutin against AGS gastric cancer cells. One key limitation is the absence of comparative controls using standard chemotherapeutic agents such as 5-fluorouracil or cisplatin, which would have enhanced the translational significance of the findings. This omission was primarily due to resource constraints, but it is acknowledged as a critical aspect for future investigations. Additionally, while molecular docking analyzes indicated favorable binding affinities of narirutin to several cancer-related targets, including LDHA, LDHB, CASP3, BAX, and NF-κB subunits, these *in silico* results were not experimentally validated using target-based assays (e.g., Western blotting, enzyme inhibition, or reporter assays). The lack of functional validation limits the mechanistic depth of interpretation and calls for further studies to confirm narirutin's direct interactions and modulatory effects on these molecular targets. In this context, our study suggests that the narirutin interactions with these proteins indicate its possible anti-inflammatory and anti-cancer effects. However, the properties stated that narirutin needs to be optimized further to improve bioavailability and membrane permeability.

Conclusion

The present study demonstrates that narirutin exerts significant cytotoxic effects against AGS gastric cancer cells, with an IC_{50} value of 43 μM, as evidenced by MTT and LDH assays. The dose-dependent reduction in cell viability, coupled with elevated LDH release, indicates a compromised membrane integrity and a strong cytotoxic potential. Moreover, AO/EB staining confirmed narirutin-induced apoptosis, showing nuclear condensation and increased apoptotic cell populations with rising concentrations. Importantly, narirutin also elevated intracellular ROS levels, suggesting that oxidative stress is a contributing mechanism of its cytotoxic and apoptotic action. This aligns with its known pro-oxidant behavior in cancer cells, which can trigger apoptosis via redox imbalance. Supporting these biological findings, the molecular docking analysis revealed high binding affinities of narirutin toward key pro-apoptotic (CASP3, BAX), inflammatory (NF-κB1, NF-κB2), and glycolytic enzymes (LDHA, LDHB). These interactions suggest potential multi-target modulation by narirutin, which may disrupt cancer cell metabolism, suppress inflammation-driven proliferation, and activate apoptotic pathways. Notably, narirutin showed the strongest binding affinity with LDHA (−9.4 kcal/mol), implicating interference with the glycolytic reprogramming commonly observed in gastric cancer (Warburg effect). While ADME/Tox profiling revealed favorable safety characteristics and aqueous solubility, poor gastrointestinal absorption and limited membrane permeability may present challenges to oral bioavailability, warranting further formulation strategies or analog development. In summary, narirutin demonstrates promising anti-gastric cancer activity through the induction of oxidative stress, apoptosis, and the disruption of metabolic and inflammatory targets. These findings support

further preclinical investigation and optimization of narirutin as a multi-targeted therapeutic candidate for gastric cancer.

Abbreviations

AGS: Human gastric cancer cell line; ANOVA: Analysis of variance; AO: Acridine orange; DCFH-DA: 2′,7′-Dichlorodihydrofluorescein diacetate; DMEM: Dulbecco's modified Eagle medium; DMSO: Dimethyl sulfoxide; EB: Ethidium bromide; FBS: Fetal bovine serum; IC_{50}: Half-maximal inhibitory concentration; LDH: Lactate dehydrogenase; MTT: 3-(4,5-Dimethylthiazol-2-yl)-2,5-diphenyltetrazolium bromide; PBS: Phosphate-buffered saline; ROS: Reactive oxygen species; SD: Standard deviation.

Declaration of Conflicting Interests

The authors declared no potential conflicts of interest with respect to the research, authorship, and/or publication of this article.

Ethical Approval

Ethical approval was obtained from the relevant ethics committee or Institutional Review Board (IRB).

Funding

The authors received no financial support for the research, authorship, and/or publication of this article.

ORCID iD

Yanling Guo https://orcid.org/0009-0000-7744-2788

References

Asiri, A., Alrehaily, A., Al Ali, A., Abu-Alghayth, M. H., & Tasleem, M. (2025). Repurposing biomolecules from *Aerva javanica* against DDX3X in LAML: A computer-aided therapeutic approach. *International Journal of Molecular Sciences*, *26*(12), 5445. https://doi.org/10.3390/ijms26125445

Bray, F., Ferlay, J., Soerjomataram, I., Siegel, R. L., Torre, L. A., & Jemal, A. (2020). Global cancer statistics 2020: GLOBOCAN estimates of incidence and mortality worldwide for 36 cancers in 185 countries. *CA: A Cancer Journal for Clinicians*, *70*(4), 313–329.

Cai, Z., Lin, J., & Zhang, L. (2018). Reactive oxygen species and cancer: The role of oxidative stress. *Antioxidants and Redox Signaling*, *28*(9), 795–811.

Chen, J., Wang, S., Wu, X., & Li, H. (2019). Narirutin: A potential natural compound for cancer prevention and therapy. *Journal of Functional Foods*, *55*, 101–110.

Czabotar, P. E., Lessene, G., Strasser, A., & Adams, J. M. (2014). Control of apoptosis by the BCL-2 protein family: Implications for physiology and therapy. *Nature Reviews Molecular Cell Biology*, *15*(1), 49–63. https://doi.org/10.1038/nrm3722

Czabotar, P. E., Westphal, D., Dewson, G., Ma, S., Hockings, C., Fairlie, W. D., Lee, E. F., Yao, S., Robin, A. Y., Smith, B. J., Huang, D. C. S., Kluck, R. M., Adams, J. M., & Colman, P. M. (2013). Bax crystal structures reveal how BH3 domains activate Bax and nucleate its oligomerization to induce apoptosis. *Cell*, *152*(3), 519–531. https://doi.org/10.1016/j.cell.2012.12.031

Eberhardt, J., Santos-Martins, D., Tillack, A. F., & Forli, S. (2021). AutoDockVina 1.2. 0: New docking methods, expanded force field, and Python bindings. *Journal of Chemical Information and Modeling*, *61*(8), 3891–3898. https://doi.org/10.1021/acs.jcim.1c00203

Elmore, S. (2007). Apoptosis: A review of programmed cell death. *Toxicologic Pathology*, *35*(4), 495–516. https://doi.org/10.1080/01926230701320337

Galluzzi, L., Bravo-San Pedro, J. M., & Kroemer, G. (2018). Organelle-specific initiation of cell death. *Nature Cell Biology*, *20*(3), 239–241.

Ganesh, P., Suresh, V., Narasimhan, M. K., & Sabarathinam, S. (2023). A narrative review on Naringin and Naringenin as a possible bioenhancer in various drug-delivery formulations. *Therapeutic Delivery*, *14*(12), 763–774. https://doi.org/10.4155/tde-2023-0086

Huang, Y., Sun, H., & Chen, S. (2017). Pharmacological properties of narirutin: An emerging flavonoid. *Phytomedicine*, *24*(12), 123–129.

Kim, S., Chen, J., Cheng, T., Gindulyte, A., He, J., He, S., Li, Q., Shoemaker, B. A., Thiessen, P. A., Yu, B., Zaslavsky, L., Zhang, J., & Bolton, E. E. (2023). PubChem 2023 update. *Nucleic Acids Research*, *51*(D1), D1373–D1380. https://doi.org/10.1093/nar/gkac956

Kolappan, S., Shen, D. L., Mosi, R., Sun, J., McEachern, E. J., Vocadlo, D. J., & Craig, L. (2015). Structures of lactate dehydrogenase A (LDHA) in apo, ternary and inhibitor-bound forms. *Acta Crystallographica Section D, Biological Crystallography*, *71*(2), 185–195. https://doi.org/10.1107/S1399004714024791

Liu, J., Han, X., Zhang, T., Tian, K., Li, Z., & Luo, F. (2023). Reactive oxygen species (ROS) scavenging biomaterials for anti-inflammatory diseases: From mechanism to therapy. *Journal of Hematology and Oncology*, *16*(1), 116. https://doi.org/10.1186/s13045-023-01512-7

Massaro, L., Raguzzini, A., Aiello, P., & Valencia, D. V. (2023). The potential role of naringin and naringenin as nutraceuticals against metabolic syndrome. *Endocrine, Metabolic and Immune Disorders—Drug Targets*, *23*(4), 428–445. https://doi.org/10.2174/1871530322666220827141203

Mishra, D., Mishra, A., & Singh, M. P. (2022). In silico insight to identify potential inhibitors of BUB1B from mushroom bioactive compounds to prevent breast cancer metastasis. *Frontiers in Bioscience*, *28*(7), 151.

Müller, C. W., Rey, F. A., Sodeoka, M., Verdine, G. L., & Harrison, S. C. (1995). Structure of the NF-κB p50 homodimer bound to DNA. *Nature*, *373*(6512), 311–317. https://doi.org/10.1038/373311a0

Munusamy, M. A., Bharathi, M., Alarfaj, A. A., Hussein-Al-Ali, S. H., Nagaiya, R., & Subbarayan, S. (2025). Glutaraldehyde-crosslinked Naringenin-loaded Albumin Nanoparticles (GNANPs) induce antimicrobial properties and apoptosis in gastric cancer cells. *Toxicology in Vitro*, 106, Article 106037. https://doi.org/10.1016/j.tiv.2025.106037

Naeem, A., Hu, P., Yang, M., Zhang, J., Liu, Y., Zhu, W., & Zheng, Q. (2022). Natural products as anticancer agents: Current status and future perspectives. *Molecules, 27*(23), 8367. https://doi.org/10.3390/molecules27238367.

Nakamura, H., & Takada, K. (2021). Reactive oxygen species in cancer: Current findings and future directions. *Cancer Science*, *112*(10), 3945–3952. https://doi.org/10.1111/cas.15068

Pachauri, S., Gupta, A., & Sharma, A. (2018). Narirutin as an anticancer agent: Molecular mechanisms and therapeutic potential. *Cancer Chemotherapy and Pharmacology*, *81*(6), 1145–1156.

Pan, W., Meshcheryakov, V. A., Li, T., Wang, Y., Ghosh, G., & Wang, V. Y.-F. (2023). Structures of NF-κB p52 homodimer-DNA complexes rationalize binding mechanisms and transcription activation. *eLife*, 12, Article e86258. https://doi.org/10.7554/eLife.86258

Prajapati, C., Rai, S. N., Singh, A. K., Chopade, B. A., Singh, Y., Singh, S. K., Haque, S., Prieto, M. A., & Ashraf, G. M. (2025). An update of fungal endophyte diversity and strategies for augmenting therapeutic potential of their potent metabolites: Recent advancement. *Applied Biochemistry and Biotechnology*, *197*(5), 2799–2866. https://doi.org/10.1007/s12010-024-05098-9

Rauf, A., Shariati, M. A., Imran, M., Bashir, K., Khan, S. A., Mitra, S., Emran, T. B., Badalova, K., Uddin, M. S., Mubarak, M. S., Aljohani, A. S. M., Alhumaydhi, F. A., Derkho, M., Korpayev, S., & Zengin, G. (2022). Comprehensive review on naringenin and naringin polyphenols as a potent anticancer agent. *Environmental Science and Pollution Research International*, *29*(21), 31025–31041. https://doi.org/10.1007/s11356-022-18754-6

Shi, D., Xu, Y., Du, X., Chen, X., Zhang, X., Lou, J., Li, M., & Zhuo, J. (2015). Co-treatment of THP-1 cells with naringenin and curcumin induces cell cycle arrest and apoptosis via numerous pathways. *Molecular Medicine Reports*, *12*(6), 8223–8228. https://doi.org/10.3892/mmr.2015.4480

Shibata, S., Sogabe, S., Miwa, M., Fujimoto, T., Takakura, N., Naotsuka, A., Kitamura, S., Kawamoto, T., & Soga, T. (2021). Identification of the first highly selective inhibitor of human lactate dehydrogenase B. *Scientific Reports*, *11*(1), Article 21353. https://doi.org/10.1038/s41598-021-00820-7

Subbarayan, S., Marimuthu, S. K., Nachimuthu, S. K., Zhang, W., & Subramanian, S. (2016). Characterization and cytotoxic activity of apoptosis-inducing pierisin-5 protein from white cabbage butterfly. *International Journal of Biological Macromolecules*, *87*, 16–27. https://doi.org/10.1016/j.ijbiomac.2016.01.072

Subbarayan, S., Subramanian, S., & Senthil Kumar, N. (2019). Recombinant pierisin-5 induces apoptosis and differential expression of Bcl-2, Bax, and p53 in human cancer cells. *DNA and Cell Biology*, *38*(8), 773–785. https://doi.org/10.1089/dna.2018.4520

Sung, H., Ferlay, J., Siegel, R. L., Laversanne, M., Soerjomataram, I., Jemal, A., & Bray, F. (2021). Global cancer statistics 2020: GLOBOCAN estimates of incidence and mortality worldwide for 36 cancers in 185 countries. *CA: A Cancer Journal for Clinicians*, *71*(3), 209–249. https://doi.org/10.3322/caac.21660

Thumpati, P., Rai, S. N., Prajapati, C., Ramakrishna, K., & Singh, S. K. (2025). Targeting c-MYC G-quadruplexes for cancer treatment with small molecules. *Scientia Pharmaceutica*, *93*(1), 6. https://doi.org/10.3390/scipharm93010006

Wang, Z., Watt, W., Brooks, N. A., Harris, M. S., Urban, J., Boatman, D., & Tomasselli, A. G. (2010). Kinetic and structural characterization of caspase-3 and caspase-8 inhibition by a novel class of irreversible inhibitors. *BiochimicaetBiophysicaActa (BBA)-Proteins and Proteomics*, *1804*(9), 1817–1831.

Wu, H., Wang, Y., Ying, M., Jin, C., Li, J., & Hu, X. (2021). Lactate dehydrogenases amplify reactive oxygen species in cancer cells in response to oxidative stimuli. *Signal Transduction and Targeted Therapy*, *6*(1), 242. https://doi.org/10.1038/s41392-021-00595-3

Xia, Y., Shen, S., & Verma, I. M. (2014). NF-κB, an active player in human cancers. *Cancer Immunology Research*, *2*(9), 823–830. https://doi.org/10.1158/2326-6066.CIR-14-0112

Youle, R. J., & Strasser, A. (2008). The BCL-2 protein family: Opposing activities that mediate cell death. *Nature Reviews Molecular Cell Biology*, *9*(1), 47–59. https://doi.org/10.1038/nrm2308

Zhang, L., Wang, J., & Liu, S. (2017). Anticancer effects of flavonoids in human cancer cells. *Frontiers in Pharmacology*, *8*, 157.

Zhou, Y., Liu, W., Wang, J., & Song, L. (2020). Narirutin induces apoptosis in hormone-refractory prostate cancer cells via caspase activation. *Journal of Natural Products*, *83*(2), 456–462.

Zhou, H., Zhang, J., & Lee, W. (2020). The role of lactate dehydrogenase in cancer therapy. *BioMed Research International*, *2020*, Article 1709403.